Formation and Rheological Properties of the Supercritical CO_2−Water Pure Interface

Frederic Tewes and Frank Boury*

Ingénierie de la Vectorisation Particulaire, INSERM U 646, Bat. IBT, 10 rue A. Boquel, 49100 Angers, France

Received: September 3, 2004; In Final Form: December 14, 2004

From the interfacial tension (γ) measurement, we have analyzed the interfacial organization that occurs between pure H_2O and pure CO_2 from a kinetical and rheological point of view. This article is the followup to a previous one, where we showed that this equilibrated interface is composed of small H_2O-CO_2 cluster blocks [Tewes, F.; Boury, F. *J. Phys. Chem. B* **2004**, *108*, 2405].[1] By analyzing the variation of γ with the square root of time, we found that the organization of the H_2O-CO_2 interface is, in the initial times, controlled by the diffusion of the CO_2 molecules into the water. We compared the frictional coefficient determined from the measured CO_2 diffusion coefficient with the frictional coefficient calculated from the Stokes equation (frictional ratio). From that, we concluded that it is a hydrated form of CO_2 that diffuses and that the degree of hydration decreases with pressure. Rheological properties of the equilibrated interface vary with CO_2 pressure, in the range of 50−90 bar, from a viscoelastic comportment to a purely elastic behavior, showing a change in the interfacial organization. The high equilibrium part of the elasticity (110 mN/m) obtained at 90 bar suggests a highly structured interface. Two phenomena could explain the interfacial rheological behavior: (i) an increase and a growth of the blocks H_2O-CO_2 cluster with the CO_2 pressure or (ii) an increase in the interfacial capacity to form stable clusters under interfacial area compression.

1. Introduction

Compressed CO_2 at a supercritical or close to a critical state has received increasing attention as an alternative to the use of toxic organic solvents in many processes such as extraction, cleaning,[2] phase transfer reactions and catalysis,[3] enzymatic catalysis,[4] and as a template in materials formation.[5] Many of these applications use CO_2 as an external phase of water-in-CO_2 microemulsions[6] or emulsions.[7,8] Therefore, interfacial tension (γ) between water and CO_2 plays an important role in the modeling and design of these processes. For instance, the droplet size and the stability of the emulsion are dependent on γ and on the characteristics of the interfacial layer. For a better understanding of the behavior of surfactant molecules at the water−CO_2 interface, and a better stabilization of water-in-CO_2 dispersion, we need to know the comportment of the pure interface in various pressure and temperature conditions.

Furthermore, the knowledge on γ between H_2O and CO_2 could help to evaluate the possibility of storage of greenhouse gases, such as CO_2, in sedimentary aquifers,[9,10] where the physical conditions are close to the critical point. Indeed, the mass transfer of the CO_2 through the water phase depends on the characteristics of the interface.

Like other physical properties, γ at the CO_2−water interface is strongly affected by the system properties near the critical point. On the other hand, very few and divergent studies concern the pure H_2O-CO_2 interface. Wilkinson and Chun[11] measured γ by means of a capillary rise method, for CO_2 pressures between 0 and 15 MPa and for different temperatures (5−71 °C). For all temperatures, they found that γ decreased with pressure until an equilibrium value close to 20 mN/m. They explained the decrease of γ with pressure as a consequence of the increase in the CO_2 solubility in the aqueous phase, forming an intermediate third phase at the interface between the CO_2 and H_2O rich phases. In Wilkinson and Chun's work, equilibrium was established very quickly with all systems. At the opposite, da Rocha et al.,[8] who used a pendant drop tensiometer, also related the decrease of γ with the CO_2 pressure until a value close to 20 mN/m. However, they additionally described a decrease of γ with time.

More recently, Hebach et al.[12] described a new apparatus allowing the measurement of γ between water and CO_2 and evidenced this pronounced dependence on pressure and temperature. Similar to da Rocha and al.,[8] they related a decrease of γ with the time and with the CO_2 pressure.

We have previously investigated the formation of water−CO_2 (W−C) pure interface by means of a drop tensiometer in which the drop area can be controlled.[1] We have described it as a two-step phenomenon. First, when a new water drop was created, the CO_2 molecules quickly adsorb onto the water surface for equilibrating their chemical potential between the bulk CO_2 and the water surface. We calculated the CO_2 molecular area at saturation and the thermodynamical parameters of the adsorption ↔ desorption equilibrium. From those values, we have found that this physisorption leads to the interaction of one CO_2 molecule with one H_2O molecule forming a H_2O-CO_2 complex of H type (Figure 1), as it was found by da Rocha et al.[13] by Monte Carlos simulation. The amount of adsorbed CO_2 and the relative orientation of H_2O and CO_2 molecules in the H type complex depend on temperature and pressure.

After this adsorption, CO_2 molecules diffuse into the water phase and then modify the water interfacial organization, which induces a kinetic effect on γ. The interfacial tension between compressed CO_2 and water depends on the number and on the energy of the interactions between CO_2 and water molecules at the interface, which depend on the organization of this interface. There are specific hydrogen bonds between the oxygen atoms

* To whom correspondence should be addressed. E-mail: boury@ibt.univ-angers.fr. Phone number: +332 41 73 58 48. Fax number: +332 41 73 58 03.

10.1021/jp046019w CCC: $30.25
Published on Web 02/10/2005

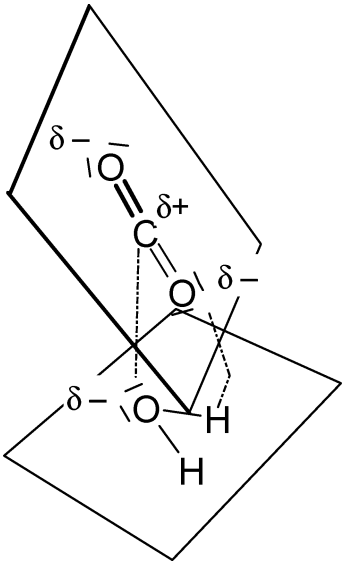

Figure 1. Possible structure of water−CO_2 interaction onto water surface: Dotted line corresponds to electrostatic interaction between the CO_2 and H_2O molecule.

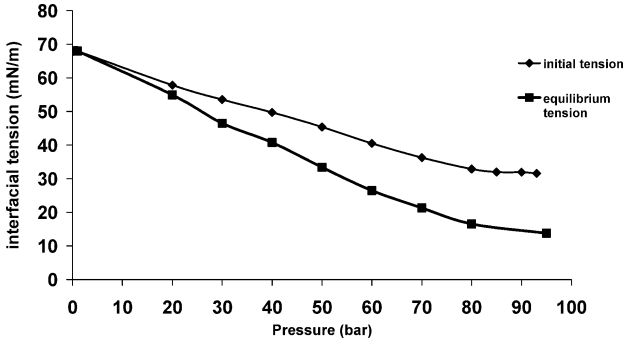

Figure 2. Equilibrium and initial interfacial tension measured at 40 °C versus CO_2 pressure, from Tewes et al.[1]

in CO_2 and the hydrogen atoms in water molecules, which allow water molecules to organize themselves. Therefore, this reorganization of the interface can create a network of H_2O-CO_2 clusters leading to a decrease of γ until an equilibrium state (Figure 2).

These H_2O-CO_2 clusters are formed at temperatures higher (20−40 °C) than the ones usually described as the limit (10 °C) for the formation of a crystalline structure, which can have few micrometers of thickness and called clathrate hydrate.[14−21] Above 10 °C (18 °C), H_2O-CO_2 clusters may be organized in a quasi-crystalline state, as it was proposed by Teng et al.[22] by interfacial macroscopic observations. This was also shown by Ohgaki et al.[23] by scanning electron microscopy. Therefore, at the temperature we performed our study, the organization of H_2O and CO_2 could be in a quasi-crystalline state. However, the thickness of the formed structure is probably smaller than at 18 °C since the apparition of a visible structure occurs only after the reduction of the drop area.

Apparent elasticity measurements and macroscopic visualization suggest that the growing of the clusters is driven by the assembling of many small blocks and accelerates with the CO_2 pressure. Their interfacial concentration and their size increase with time until an equilibrium state. From CO_2 pressures of 80 bar, at the equilibrium state, the interface is saturated with cluster blocks.[1]

CO_2-H_2O clusters structure and formation depend on thermodynamic properties, such as temperature and pressure. In contrast, the aggregation of the cluster blocks at the interface and subsequently the rheological behavior of the interfacial layer, depend on mechanical properties such as cluster block size and adhesion force between the blocks.

To better understand the formation mechanism of the H_2O-CO_2 interface, we analyze the variation of γ with time. Furthermore, to increase the knowledge on the clusters aggregation at the H_2O-CO_2 interface, and then, to understand how these clusters could interact with surfactant molecules, we present in this paper the first interfacial rheology study in a supercritical medium. These measurements allow us to describe and know how these clusters interact at different CO_2 pressures.

2. Materials and Methods

Pendant Drop Tensiometer. The drop tensiometer (Tracker, IT Concept, France) allows for the determination of the interfacial tension by analyzing the axial symmetric shape (Laplacian profile) of the pendant drop (aqueous phase) in CO_2. The apparatus consists of a view cell under CO_2 atmosphere, a light source, a CCD camera, a computer, a syringe (Exmire microsyringe MS*GLL100, ITO corporation, Japan), and a motor as described by Tewes et al.[1] The syringe was filled with pure water and coupled to the view cell. Then, the view cell was pressurized with pure CO_2 until reaching the desired temperature (40 °C) and pressure. After that, the system is left during 24 h for equilibrating the water phase with the CO_2 phase. Pendant drops whose area is controlled during the whole time of experience by the motor were formed at the end of a stainless steel needles (needles 20G, popper, U.S.A.), having an inside diameter of 1 mm and connected to the syringe. The interfacial tension is determined by first digitizing and analyzing the profile of the droplet using a CCD camera coupled to a video image profile digitizer board connected to the computer.[24] The measurements were performed at pressures ranging from 30 to 90 bar, corresponding respectively to densities of 59 and 486 kg/m^3.

Rheological Measurements. The common idea of all of the related rheological experiments is to apply a controlled perturbation to the surface in order to simultaneously follow the related surface pressure variations.

The dynamic response of a surface film to a dilatational mechanical stress in the time scale of $1-10^3$ s is studied by means of a ramp type perturbation approach. This approach consists of realizing two types of continuous and monotonic compressions of the equilibrated surface layer on a pendant drop: a slow compression (dashed line) and fast compression (bold line) (Figure 3b). Simultaneously, we record the variation of the interfacial pressure during the slow compression (dashed line) or after the fast compression to measure the relaxation of the interface (bold line) (Figure 3a).

In this case, a convenient theoretical model (generalized Maxwell; Figure 4), corresponding to a solid viscoelastic body, has been developed and applied to many kinds of interfacial systems (phospholipids or polymers).[25−28]

To describe the total surface pressure change $\Delta\pi = \pi(t) - \pi_i$ (i.e., resulting stress; with π_i equal to the initial surface pressure before the compression (Figure 3a)) during the time t_c of the slow compression performed at a constant velocity U_b, we supposed that at any moment it can be written as a sum of an equilibrium ($\Delta\pi_e$) and an nonequilibrium ($\Delta\pi_{ne}$) contributions of stress

$$\Delta\pi = \Delta\pi_e + \Delta\pi_{ne} \quad (1)$$

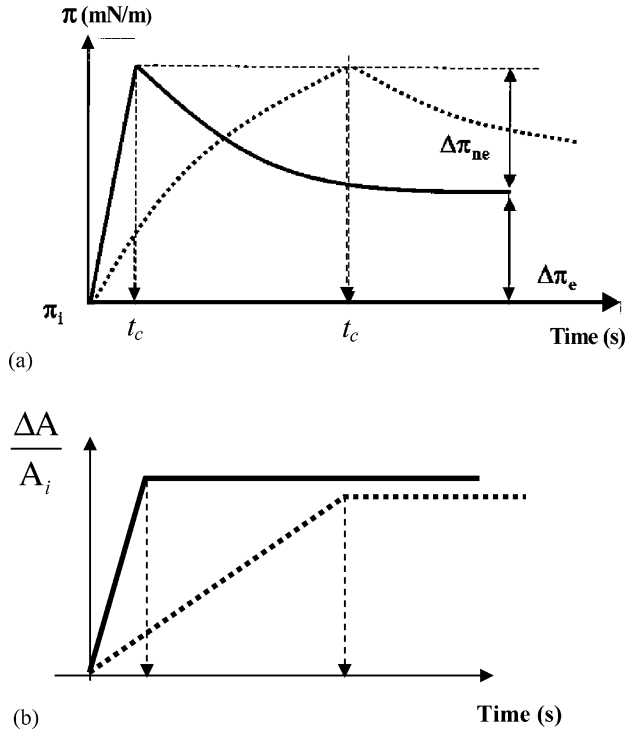

Figure 3. (a) Surface pressure change $\Delta\pi$ during the time t_c; (b) relative area compression. (Bold line: fast compression; dashed line: slow compression).

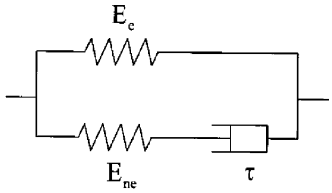

Figure 4. Generalized Maxwell mechanical model.

The equilibrium part of the resulting stress $\Delta\pi_e$ depends on the equilibrium surface dilatational elasticity E_e

$$\Delta\pi_e = E_e\frac{U_b t}{A_i} \tag{2}$$

where A_i is the initial surface area before the mechanical strain

$$\frac{U_b t}{A_i} \equiv \frac{\Delta A}{A_i} \tag{3}$$

This elastic behavior is represented by the upper branch of the mechanical model in Figure 4. The nonequilibrium part of the resulting stress $\Delta\pi_{ne}$ is correlated to the accumulation of elastic energy during the compression. The dissipation of this accumulated energy occurs during the compression as well as the relaxation and can be interpreted as a molecular reorganization in the interface. This viscoelastic behavior can be described using the following equation:

$$\frac{d\Delta\pi_{ne}}{dt} + \frac{\Delta\pi_{ne}}{\tau} = E_{ne}\frac{U_b}{A_i} \tag{4}$$

where E_{ne} is the nonequilibrium surface dilatational elasticity and τ is the specific time of relaxation. The viscoelastic behavior is represented by the lower branch of the mechanical model in

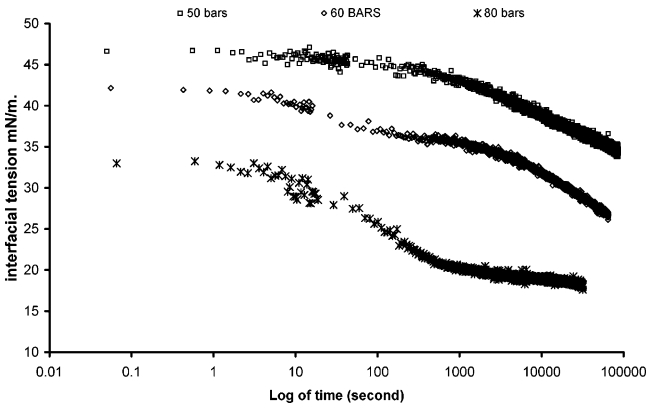

Figure 5. Kinetics of the decrease of γ for different CO_2 pressure.

Figure 4. If the initial conditions are $\Delta\pi_{ne} = 0$ at $t = 0$, $\Delta\pi_{ne}$ can be written:

$$\Delta\pi_{ne} = \frac{E_{ne}U_b t}{A_i}(1 - e^{-t/\tau}) \tag{5}$$

The two branches of the mechanical model are coupled in parallel according to eq 1 corresponding to the additivity of stresses; we obtained the following equation describing the viscoelastic behavior of the monolayer

$$\frac{\Delta\pi}{U_b t}A_i = E_e + E_{ne}\frac{\tau}{t}(1 - e^{-t/\tau}) \tag{6}$$

The specific time of relaxation process τ was easily determined from experiments where the time of compression t_c was much smaller than it (fast compression). This time τ is then injected in eq 6 against the time t of the slow compression. Using the experimental values found for $\Delta\pi(t)$ obtained during the slow compression and with eq 6, it is possible to determine the nonequilibrium part (E_{ne}) and the equilibrium part (E_e) of the dilatational elasticity.

For the determination of E_e, E_{ne}, and τ, one has to successively perform the following:

•Fast compression ($d/dt\ \Delta A(t)/A_i = U/A_i$ typically higher than 0.005 s^{-1}, with $\Delta\pi$ typically lower than 2 mN/m) in order to determine more precisely the relaxation time τ. Subsequently, this characteristic time of relaxation is determined by fitting the γ relaxation curves by an exponential equation: $\gamma = \gamma_\infty + Ae^{-(t/\tau)}$).

•Slow compression ($d/dt\ \Delta A(t)/A_i = U/A_i$ typically lower than 0.003 s^{-1}) (with $\Delta\pi < 2$ mN/m) in order to determine the compression relaxation part. The value of τ and eq 5 are used to determine E_e and E_{ne}.

3. Results and Discussion

3.1. Kinetics. The interfacial tension between pure CO_2 and pure water is shown in Figure 5 versus the logarithm of time for a temperature of 40 °C and for different CO_2 pressures.

As already described by Tewes and Boury,[1] γ between the two pure phases decreases until an equilibrium value. From 30 to 80 bar, higher the CO_2 pressure, higher the magnitude of the decrease.

The kinetics can be well fitted with a exponential equation having three characteristics times T_1, T_2, and T_3. These times are dependent on the CO_2 pressure: the higher the pressure, the lower the characteristic times (Table 1).

The variation of γ with time is attributed to the reorganization of the interface after the adsorption of CO_2 molecules onto the

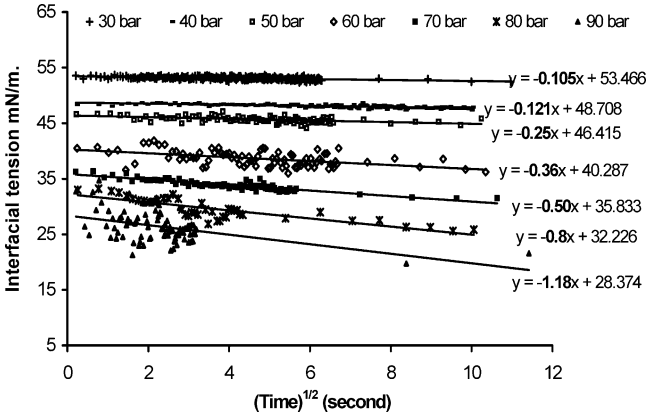

Figure 6. Interfacial tension versus $\sqrt{t}$ for various CO_2 pressures at 40 °C.

TABLE 1: Characteristic Times Describing the γ Kinetics

CO_2 pressure (bar)	T_1 (s)	T_2 (s)	T_3 (s)
50	49.9	6000	70000
60	27.7	4050	38385
70	20	2570	26000
80	9.5	300	13800
90	0.7	36	1000

H_2O drop surface.[1] In these conditions, an interphase having a given thickness is formed, which can results from the diffusion of the CO_2 and water molecules in the opposite phase. Therefore, the values of the first characteristic time can be attributed to three phenomena: (i) the diffusion of the CO_2 from the water surface into the water phase, (ii) the diffusion of water into the CO_2 phase, and (iii) the nucleation of the H_2O-CO_2 cluster. The other characteristic times can be associated to the growth and the aggregation of the cluster in blocks.

Among these three phenomena, the one responsible for the value of the first characteristic time is the slowest (limiting step). The diffusion of water in CO_2 can be assumed to be fast due to the relatively high diffusion coefficient of water in CO_2: 2.8×10^{-8} m^2 s^{-1} at 35 °C and 135 bar,[29] and to be of low intensity due to the low solubility of water in CO_2 phase under these conditions (<0.1 mol %).[22] Therefore, the diffusion of water in CO_2 should not be the phenomenon which controls the reorganization of the interface.

To determine which step is the limiting one (cluster nucleation or CO_2 diffusion) controlling the values measured for the first characteristic time, we tried to determine the diffusion coefficient of CO_2 into the water from the γ values, by plotting γ versus $\sqrt{t}$ for different CO_2 pressures (Figure 6).

The fact that γ decreases linearly with the root square of time generally suggests that the kinetics is controlled by a diffusion mechanism.[30]

The usual equation that simply describes the variation of γ with time as a diffusion controlled mechanism accounts for the diffusion of tensioactive molecules from the bulk phase to the interface, and also the back diffusion from the interface to the bulk phase.[31]

Here, we want to describe the diffusion of CO_2 molecules from the initial water plane to a new hypothetical plane situated in the interphase (layer with the thickness of a few molecules; ~0.8 nm),[13] leading to its reorganization (less defined interface) and to a decrease of the interfacial tension (Figure 7).

At the start of the diffusion process, back diffusion of CO_2 can be neglected because very few CO_2 molecules are present in the water bulk due to their relatively low solubility,[13,32] and limiting laws can be used to describe the variation of γ with time. Therefore, the simplified Ward and Tordai equation

$$\Gamma_t = 2C\sqrt{\frac{D_{CO2}t}{\pi}} \qquad (7)$$

where C is the bulk CO_2 concentration (mole/m^3, equal to $C \equiv$

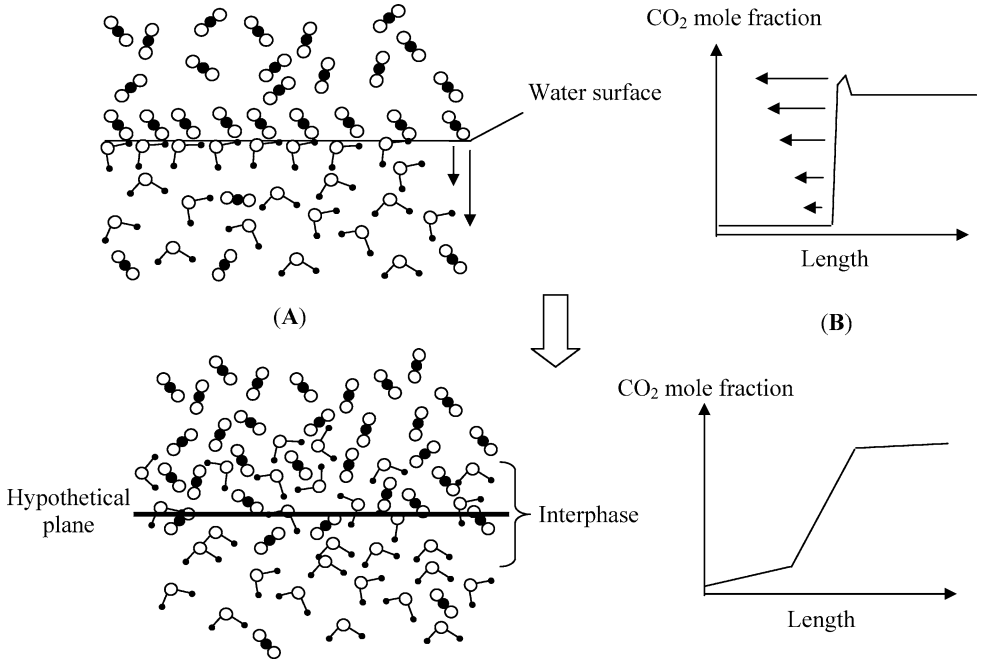

Figure 7. Schematic illustration of new interphase creation. (A) At the top, molecular representation of the interface, which is created in the initial time: CO_2 molecules are adsorbed onto the water surface saturated with CO_2 to form a well delimited interface where H_2O and CO_2 form a H type complex from CO_2 pressure higher than 70 bar. At the bottom, CO_2 molecules have diffused within few angstroms into the water phase to create a less delimited interphase where the water is supersaturated in CO_2. (B) At the top, representation of the variation of the CO_2 mole fraction trough the interface. The interfacial thickness is short, and the crop on the curve symbolizes the excess of CO_2 molecules adsorbed onto the water surface. At the bottom, the interface is became an interphase, less delimited and with a larger thickness.

TABLE 2: CO_2 Diffusion Coefficients in Water at 40°C in Function of CO_2 Pressures

CO_2 pressure (bar)	D_{CO2} (m^2/s)	standard deviation (m^2/s)
30	7.2×10^{-10}	$\pm 7.8 \times 10^{-10}$
40	4.7×10^{-10}	$\pm 5.1 \times 10^{-11}$
50	1.1×10^{-9}	$\pm 5.1 \times 10^{-10}$
60	1.5×10^{-9}	$\pm 6.8 \times 10^{-10}$
70	1.7×10^{-9}	$\pm 2.5 \times 10^{-10}$
80	1.8×10^{-9}	$\pm 4.5 \times 10^{-10}$
90	1.3×10^{-9}	$\pm 9.6 \times 10^{-10}$

ρ_{CO2}/M_{CO2}), D_{CO2} is the CO_2 diffusion coefficient (m^2/s) and $\pi = 3.142$, can be used and associated to an appropriate isotherm which links Γ (mole/m^2) and γ (N/m), like the linear Henry isotherm

$$\gamma = \gamma_0 - nRT\Gamma \tag{8}$$

which finally gives

$$\gamma_t = \gamma_0 - 2RTC\sqrt{\frac{D_{CO2}}{\pi}}\sqrt{t} \tag{9}$$

The values of D_{CO2} versus CO_2 pressure are represented in Table 2. We can notice important values for the absolute standard deviations of D_{CO2}, due to the low values of D_{CO2}. Furthermore, these values of D_{CO2} are on the same order of magnitude as those determined by other techniques. For instance, Liger-Belair et al.,[33] found by NMR a value of 1.85×10^{-9} m^2 s^{-1} in the fizzy water at 20 °C and under atmospheric pressure. Hirai *et* al.[34] determine the CO_2 diffusion coefficient in water at 294 and 392 bar for a temperature of 13 °C by measuring the rate of volume decrease of the CO_2 droplet formed into the water phase and found a value close to 1.3×10^{-9} m^2 s^{-1}. The linearity of the decrease of γ with the square root of time, and the values of D_{CO2}, close to those found for the CO_2 dissolved in water, suggest that the limiting step controlling the characteristic time T_1 of the γ kinetics is the diffusion of CO_2 in the water phase. Consequently, the initial reorganization of the water molecules induced by the presence of CO_2 molecules, i.e., clusters nucleation, should be faster and masked by the CO_2 diffusion phenomena. Uchida et al.[14] observed similar phenomena for the H_2O-CO_2 clathrate formation and showed that the nucleation rate was faster than the CO_2 diffusion rate.

However, the D_{CO2} values cited by the two above studies are measured at temperatures lower than ours, so for a unique CO_2 molecule, we should find slightly higher values than those measured by these two studies. Furthermore, Table 1 indicates that our D_{CO2} values increase with the CO_2 pressure. To explain the variation of the D_{CO2} values with the CO_2 pressure and the fact that our D_{CO2} are slightly lower relative to the other studies, we compared the values of the frictional coefficient *f*, obtained from the measured D_{CO2} by using the Stokes−Einstein equation

$$f = \frac{k_B T}{D_{CO2}} \tag{10}$$

where k_B is the Boltzmann constant and *T* the temperature, with the frictional coefficient f_0 obtained from the Stokes equation

$$f_0 = 6\pi\eta R \tag{11}$$

where η is the viscosity of water at 40 °C, saturated with CO_2,[35] and *R* is the radius of a CO_2 molecule, which is assimilated to a hard sphere. However, the CO_2 is not spherical and its frictional coefficient is larger than if we consider CO_2 as a spherical molecule of the same volume, because there will be a larger surface contact with the solvent and this will increase the hydrodynamic drag.

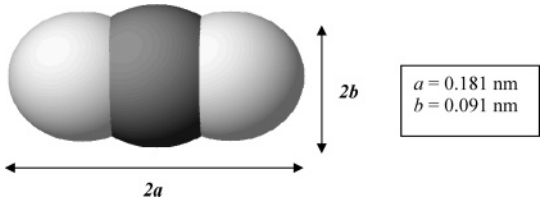

Figure 8. Schematic representation of CO_2 molecules with its characteristic dimensions.[33]

Therefore, we can use some simple considerations to calculate the frictional coefficient considering the CO_2 as a cylinder-like molecule. For a cylindrical molecule having a length equal to $2a$ and a radius equal to b (Figure 8), the frictional coefficient can be defined as

$$f_0 = f_R \frac{(2/3)^{1/3} P^{2/3}}{Ln2P - 0.3} \tag{12}$$

The term f_R in this equation is defined as $f_R = 6\pi\eta R_0$, where R_0 is equal to $3ab^2/2$ and defined as the radius of a sphere that has a volume equal to the volume of a cylinder having an axial ratio $P = a/b$. The rest of the expressions accounts for a "shape" correction, i.e., represents the effect of the particular cylinder shape on diffusion. The value of this frictional coefficient is intermediate between frictional coefficients calculated by considering the CO_2 as a hard sphere having a radius equal to the lower length of the CO_2 *b* and the one calculated with the larger dimension *a*.

The difference between the values of *f* and f_0 can be explained by several phenomena such as the degree of hydration of the CO_2 or a dynamic aggregation process between the unhydrated or hydrated CO_2 molecules, which increases the size of the diffusive species.

Therefore, from the comparison of the values of *f* with f_0, we can determine the degree of hydration of the CO_2 by considering that no other phenomena induce an increase of *f*. In fact, f_0 can be defined as the frictional coefficient expected for an unhydrated CO_2. If *f* is obtained for a hydrated form, then the frictional ratio f/f_0 is equal to the ratio of the radius *R* of a sphere having a volume V_H equivalent to the total hydrodynamic volume including hydration, under the radius R_0 of a sphere having the volume V_{CO2} of a free CO_2 molecule (eq 13)

$$\frac{f}{f_0} = \frac{R}{R_0} \tag{13}$$

Total hydrodynamic volume V_H can be described as the free CO_2 volume plus *x* times H_2O molecular volume

$$V_H = V_{CO2} + xV_{H2O} \tag{14}$$

Therefore $V_H = 4\pi/3((f/f_0)R_0)^3 = V_{CO2} + xV_{H2O} = 2a\pi b^2 + x((4\pi/3)R_{H2O}{}^3)$, with R_{H2O} equal to 0.096 nm. The results are summarized in Table 3.

Table 3 shows that for all the CO_2 pressures *f* is higher than f_0. This difference decreases when the CO_2 pressure increases. For the CO_2 pressures between 60 and 80 bar, the calculation of the number of water molecules linked to one CO_2 molecule leads to plausible values. For instance, at 80 bar, one water molecule is associated with one CO_2 molecule. This result

TABLE 3: Frictional Coefficients and Total Hydrodynamic Volume

CO_2 pressure	f (g/s)	f_0 (g/s)	f/f_0	V_H (m^3)
30	6.0×10^{-9}	2.06×10^{-9}	2.91	2.32×10^{-28}
40	9.2×10^{-9}	2.06×10^{-9}	4.47	8.39×10^{-28}
50	3.9×10^{-9}	2.06×10^{-9}	1.91	6.56×10^{-29}
60	2.8×10^{-9}	2.06×10^{-9}	1.37	3.88×10^{-29}
70	2.5×10^{-9}	2.06×10^{-9}	1.21	2.98×10^{-29}
80	2.4×10^{-9}	2.06×10^{-9}	1.15	1.45×10^{-29}
90	3.2×10^{-9}	2.06×10^{-9}	1.57	3.65×10^{-29}

suggests that it is a hydrated form of CO_2 that diffuses from the water surface into the water phase and induces the interfacial reorganization. The calculation of f by considering the CO_2 as a hard sphere having a radius equal to its maximal length, a in Figure 8, gives a similar conclusion. This result is in accordance with a previous study where we showed that, from a CO_2 pressure of 80 bar, the water surface is saturated with CO_2 and forms a 1/1 H_2O-CO_2 complex of H type.[1] So, one can suggest that it is this complex that diffuses in this range of pressures and that, at lower CO_2 pressure, it is a more hydrated CO_2 form that diffuses, explaining the lower obtained D_{CO2}.

Unfortunately, the too low precision on the values of D_{CO2} makes difficult the calculation of the values of the number of water molecules associated with a CO_2 molecule. Furthermore, the calculation of the number of water molecules linked to one CO_2 molecule from the data acquired at low CO_2 pressures leads to values higher than the maximal one, which is 4 H_2O/1 CO_2.[36] Therefore, it can be supposed that another phenomenon reduces the CO_2 diffusion coefficient lower than the one expected for the diffusion of a hydrated CO_2 form. One possible interpretation of these data is that, at low CO_2 pressure, hydrated forms of CO_2 are involved in dynamic association processes, increasing the frictional coefficient value. At 90 bar, the important error on the calculation of D_{CO2} leads to the impossibility of giving any conclusion on the degree of hydration of the CO_2 molecules.

3.2. Rheology. We have first measured the apparent dilatational elasticity ($E_a = (\Delta\gamma/\Delta A)A_i$) of the equilibrated interfacial layer by slowly reducing the drop area (strain) and then measuring the resulting change of γ (stress) for various CO_2 pressures (Figure 9). This elasticity depends on the rate of the decrease in area due to viscoelastic effect, so we have always performed the measurement at the same decrease rate. For the lowest CO_2 pressures, E_a is low (~10 mN/m), indicating a low cohesivness of the interface. By increasing the CO_2 pressure until 90 bar, E_a monotonically increases until values around 110 mN/m, showing a rigid structurated interface. The high value of E_a obtained at 90 bar, illustrates a high degree of interaction in the plane of the interface.

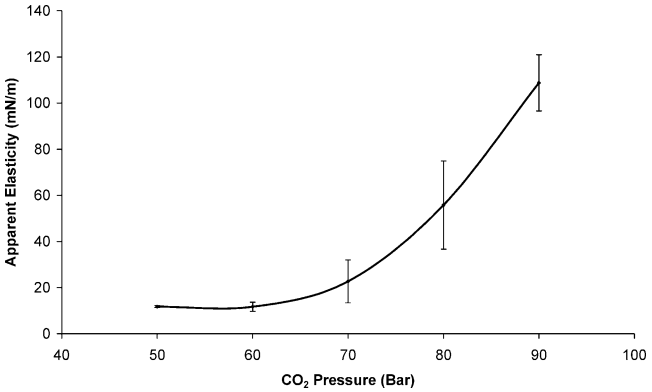

Figure 9. Apparent elasticity of the equilibrated water−CO_2 pure interface versus CO_2 pressure (40 °C).

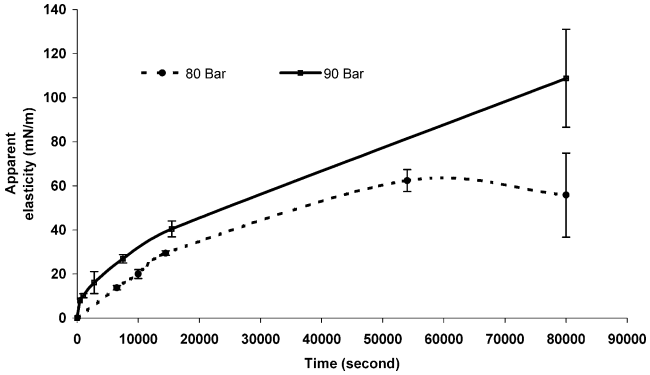

Figure 10. Apparent elasticity versus time for the CO_2 pressure of 80 and 90 bar and a temperature of 40 °C.

The variation of E_a with time is shown in Figure 10. For 90 bar, E_a fastly increases in the earlest times (500 s), which could be attributed to the formation of H_2O-CO_2 clusters block, and then it increases more slowly that could be attributed to the growth and aggregation of the blocks.

For a more precise analysis of the quality of the interface, we have measured the dilatational rheological parameters of the interfacial layer. The apparent elasticity is composed of a pure elastic part E_e related to the conservation of the energy and a viscoelastic part E_{ne}, which is linked to the dissipation of the energy due to a reorganization of the interface during or after the compression, depending on the characteristic times.

In the range of 50−70 bar, the pure interface has mainly a viscoelastic behavior, with a significant E_{ne} value. Above 70 bar, the rheological comportement of the interface changes to become purely elastic. This rheological behavior can be explained by two possible phenomena.

The first explanation is a structuration of the interface, with an increase in the size and the interfacial concentration of the cluster blocks. In fact, the viscoelastic behavior obtained between 50 and 70 bar can be explained by the structure of the interface with the presence of a small number of cluster blocks, surrounded by a phase made of less organized structures. This type of organization has also been observed on hydrochlorofluorocarbon clathrate growth on a glass window by Mochizuki,[37] who often observed small areas not covered with hydrate crystals and surrounded by crystal plates. They explained this phenomenon by the anisotropic growth of the hydrate-crystal plates. The decrease of the E_{ne} part of the elasticity with the CO_2 pressure indicates a structuration of the interface and a lowering of the dynamic effects linked to the interaction between the cluster blocks; that is, the interface becomes saturated with cluster blocks.

When the area is compressed faster than the characteristic rate of the cluster blocks displacement (fast compression), some blocks aggregate. If the interface is not saturated, the cluster blocks have enough place for their desaggregation and their homogeneous spreading on the interphase (Figure 12). This situation leads to the viscoelastic comportement obtained for CO_2 pressures lower than 80 bar.

On the contrary, when the interface is saturated with blocks, clusters have no place for their spreading and a pure elastic comportement as for CO_2 pressures of 80 and 90 bar is obtained. The high elasticity values obtained for the pCO_2 of 80 and 90 bar (Figure 11), which can be compared to a solidlike behavior, reveal strong lateral interactions between the H_2O-CO_2 clusters at these pressures. The increase of E_e recorded from 80 to 90 bar shows an increase in the degree of these interactions.

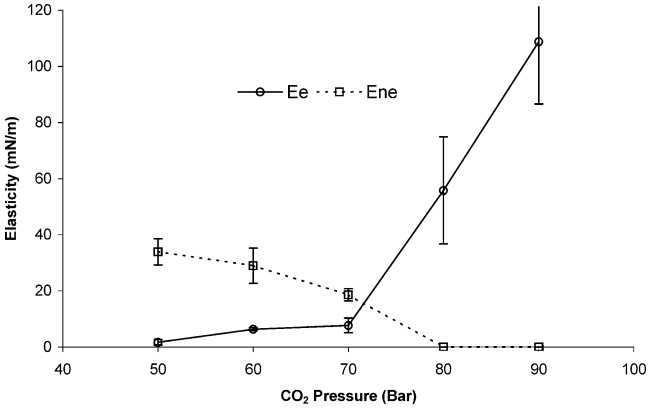

Figure 11. Evolution of the equilibrium (E_e) and nonequilibrium (E_{ne}) elasticity of pure water−CO_2 equilibrated interface versus CO_2 pressure.

The second explanation is that the H_2O-CO_2 cluster block formation occurs under compression of the area; that is, the supersaturated interphase is structurated when the drop area decreases. The viscoelastic behavior obtained between 50 and 70 bar can be explained by a too low CO_2 supersaturation of the interphase and the instability of the new formed cluster blocks. When the area is reduced, local supersaturation occurs leading to the formation of cluster blocks. The following relaxation phenomenon is due to the breaking of the blocks because of a homogenization of the CO_2 concentration in the interphase. A decrease of E_{ne} when the CO_2 pressure increases is due to an increase in the interphase supersaturation. From 80 bar, the interphase is enough supersaturated to give stable clusters which fill the interphase.The increase of E_e between 80 and 90 bar is the consequence of an increase in the number of formed clusters and in the interaction between them.

4. Conclusion

The analysis of the first time of the γ kinetics obtained at various CO_2 pressures allowed us to determine that the diffusion of the CO_2 into the water controls the interfacial organization that occurs between the pure water and pure carbon dioxide. The ratio between the frictional coefficient calculated from the measured D_{CO2} and the theoretical frictional coefficient calculated by taking into account the cylindrical shape of the CO_2 molecule, suggests that it is a hydrated form of CO_2 that diffuses. Furthermore the degree of hydration would decrease when the CO_2 pressure increases.

Rheological properties of the interface vary with the CO_2 pressure from a viscoelastic behavior obtained between 50 and 70 bar, to a purely elastic behavior, characterized by high elasticity values, in the range of 80−90 bar. This change in the rheological behavior with the CO_2 pressure could be due to two hypothetical phenomena. First, an increase in the interface organization formed of solidlike H_2O-CO_2 cluster blocks. This leads to an increase of the size and/or the concentration of the clusters in the interphase. As a matter of fact, an increase in CO_2 pressure causes a large change in the interfacial H_2O structure.[13] Second, the rheological behavior changes with pressure could be linked to the increase in the CO_2 supersaturation in the interphase. This local supersaturation could enhance the capacity to form H_2O-CO_2 clusters under surface compression. Kinetical and rheological behaviors play an important role on the adsorption of surfactant molecules at the H_2O/CO_2 interface. Consequently, the organization of water and CO_2 molecules during such dynamic processes should probably be taken into account. This is probably crucial at low surfactant concentrations as it was observed with proteins.[38] In all cases, much more information could be obtained on the organization of this peculiar interface by in situ structural analysis, carried out for instance by RAMAN spectroscopy measurement.[39]

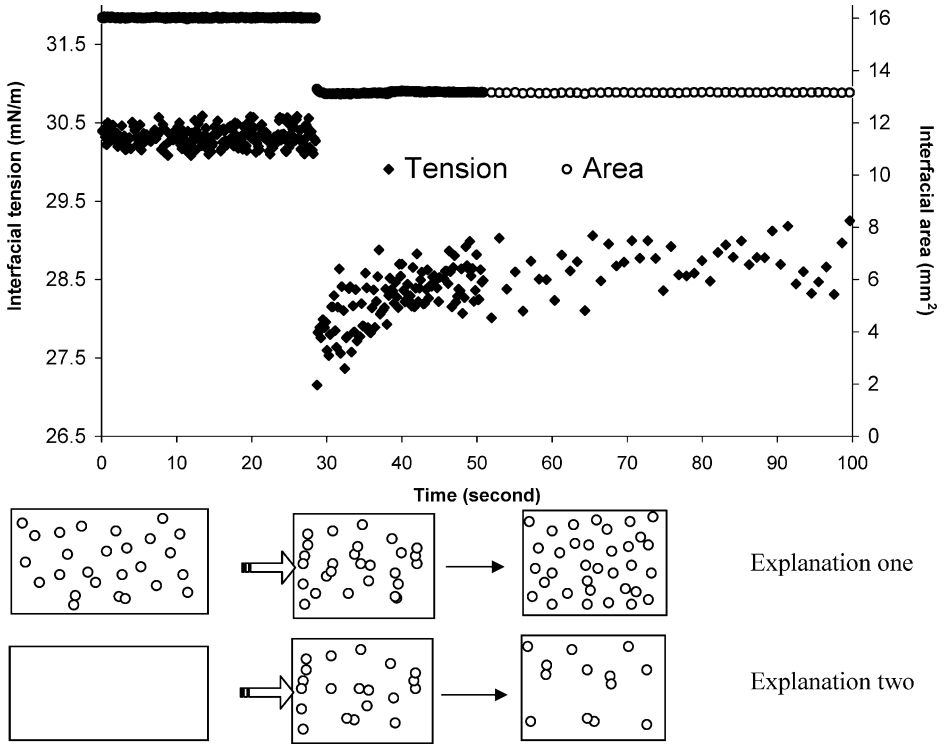

Figure 12. Scheme of the surface morphology variation during a compression−relaxation process.

References and Notes

(1) Tewes, F.; Boury, F. *J. Phys. Chem. B* **2004**, *108*, 2405.

(2) Campbell, M. L.; Apodaca, D. L.; Yates, M. Z.; McCleskey, T. M.; Birnbaum, E. R. *Langmuir* **2001**, *17*, 5458.

(3) Jacobson, G. B.; Ted Lee Jr., C.; Johnston, K. P.; Tumas, W. *J. Am. Chem. Soc.* **1999**, *121*, 11902.

(4) Kane, M. A.; Baker, G. A.; Pandey, S.; Bright, F. V. *Langmuir* **2000**, *16*, 4901.

(5) Holmes, J. D.; Bhargava, P. A.; Korgel, B. A.; Johnston, K. P. *Langmuir* **1999**, *15*, 6613.

(6) Eastoe, J.; Cazelles, B. M. H.; Steytler, D. C.; Holmes, J. D.; Pitt, A. R.; Wear, T. J.; Heenan, R. K. *Langmuir* **1997**, *13*, 6980.

(7) Ted Lee, C. J.; Psathas, P. A.; Johnston, K. P.; deGrazia, J.; Randolph, T. W. *Langmuir* **1999**, *15*, 6781.

(8) da Rocha, S. R. P.; Harrison, K. L.; Johnston, K. P. *Langmuir* **1999**, *15*, 419.

(9) Xu, T.; Apps, J. A.; Pruess, K. *Appl. Geochem.* **2004**, *19*, 917.

(10) Caron, F.; Manni, G.; Workman, W. J. G. *J. Geochem. Explor.* **1998**, *64*, 111.

(11) Chun, B.-S.; Wilkinson, G. T. *Ind. Eng. Chem. Res.* **1995**, *34*, 4371.

(12) Hebach, A.; Oberhof, A.; Dahmen, N.; Kögel, A.; Ederer, H.; Dinjus, E. *J. Chem. Eng. Data* **2002**, *47*, 1540.

(13) da Rocha, S. R. P.; Johnston, K. P.; Westacott, R. E.; Rossky, P. J. *J. Phys. Chem. B* **2001**, *105*, 12092.

(14) Uchida, T.; Ebinuma, T.; Kawabata, J. i.; Narita, H. *J. Cryst. Growth* **1999**, *204*, 348.

(15) Mori, Y. H. *Energy Convers. Manage.* **1998**, *39*, 1537.

(16) Uchida, T. *Waste Manage.* **1998**, *17*, 343.

(17) Hirai, S.; Okazaki, K.; Tabe, Y.; Hijikata, K.; Mori, Y. *Energy* **1997**, *22*, 285.

(18) Hirai, S.; Okazaki, K.; Tabe, Y.; Kawamura, K. *Energy Convers. Manage.* **1997**, *38*, S301.

(19) Hirai, S.; Okazaki, K.; Araki, N.; Yazawa, H.; Ito, H.; Hijikata, K. *Energy Convers. Manage.* **1996**, *37*, 1073.

(20) Mori, Y. H.; Mochizuki, T. *Energy Convers. Manage.* **1998**, *39*, 567.

(21) Tabe, Y.; Hirai, S.; Okazaki, K. *J. Cryst. Growth* **2000**, *220*, 180.

(22) Teng, H.; Yamasaki, A. *Int. J. Heat Mass Transfer* **1998**, *41*, 3204.

(23) Ohgaki, K.; Kirokawa, N.; Ueda, M. *Chem. Eng. Sci.* **1992**, *47*, 1819.

(24) P. Saulnier, F. B., A. Malzert, B. Heurtault, Tz. Ivanova, A. Cagna, I. Panaýïotov, and J. E. Proust. *Langmuir* **2001**, *17*, 8104.

(25) Boury, F.; Ivanova, T.; Panaieotov, I.; Proust, J. E.; Bois, A.; Richou, J. *Langmuir* **1995**, *11*, 1636.

(26) Boury, F.; Ivanova, T.; Panaiotov, I.; Proust, J. E.; Bois, A.; Richou, J. *J. Colloid Interface Sci.* **1995**, *169*, 380.

(27) Doisy, A.; Proust, J. E.; Ivanova, T.; Panaïotov, I.; Dubois, J. L. *Langmuir* **1996**, *12*, 6098

(28) Panaiotov, I.; Ivanova, T.; Proust, J.; Boury, F.; Denizot, B.; Keough, K.; Taneva, S. *Colloids Surf. B: Biointerfaces* **1996**, *6*, 243.

(29) Xu, B.; Nagashima, K.; DeSimone, J. M.; Johnson, C. S. *J. Phys. Chem. A* **2003**, *107*.

(30) Danov, K. D.; Kolev, V. L.; Kralchevsky, P. A.; Broze, G.; Mehreteab, A. *Langmuir* **2000**, *16*, 2942.

(31) Eastoe, J.; Dalton, J. S. *Adv. Colloid Interface Sci.* **2000**, *85*, 103.

(32) Bando, S.; Takemura, F.; Nishio, M.; Hihara, E.; Akai, M. *J. Chem. Eng. Data* **2003**, *48*, 576.

(33) Liger-Belair, G.; Prost, E.; Parmentier, M.; Jeandet, P.; Nuzillard, J.-M. *J. Agric. Food Chem.* **2003**, *51*, 7560.

(34) Hirai, S.; Okazaki, K.; Yazawa, H.; Ito, H.; Tabe, Y.; Hijikata, K. *Energy* **1997**, *22*, 363.

(35) Bando, S.; Takemura, F.; Nishio, M.; Hihara, E.; Akai, M. *J. Chem. Eng. Data* **2004**, *49*, 1328.

(36) Nguyen, M. T.; Raspoet, G.; Vanquickenborne, L. G.; Duijnen, P. T. V. *J. Phys. Chem. A* **1997**, *101*, 7379.

(37) Mochizuki, T. *J. Cryst. Growth* **2003**, *249*, 372.

(38) Tewes, F.; Boury, F.; Cagna, A. "Effect of H_2O−CO_2 organization on ovalbumin adsorption at the supercritical CO_2-water interface"; 7th Italian Conference on Supercritical Fluids and their Applications, 2004, Trieste (Italy).

(39) Sum, A. K.; Burruss, R. C.; Sloan Jr., E. D. *J. Phys. Chem. B* **1997**, *101*, 7371.